Surface reconstructions of epitaxial MnAs films grown on GaAs(111)B

A. Ouerghi, Massimiliano Marangolo, Mahmoud Eddrief, B. Lipinski, Victor H. Etgens, M. Lazzeri, H. Cruguel, F. Sirotti, A. Coati, Yves Garreau

Surface reconstructions of epitaxial MnAs films grown on GaAs(111)B

A. Ouerghi,[1,*] M. Marangolo,[1] M. Eddrief,[1] B. B. Lipinski,[1,†] V. H. Etgens,[1] M. Lazzeri,[2] H. Cruguel,[3] F. Sirotti,[3,4] A. Coati,[3,4] and Y. Garreau[3,4,5]

[1]*Institut des NanoSciences de Paris, INSP, Université Pierre et Marie Curie–Paris 6, Université Denis Diderot–Paris 7, CNRS, UMR 7588 Campus Boucicaut, 140 rue de Lourmel, 75015 Paris, France*

[2]*Institut de Minéralogie et de Physique des Milieux Condensés, IMPCM, Université Pierre et Marie Curie–Paris 6, CNRS, UMR 7590, case 115, 4 place Jussieu, F75252 Paris-Cedex 05, France*

[3]*Laboratoire pour l'Utilisation du Rayonnement Electromagnétique (LURE), Centre Universitaire Paris Sud, BP 34, F-91898 Orsay, France*

[4]*Synchrotron SOLEIL, L'Orme des Merisiers, Saint-Aubin, BP 48, 91192 Gif-sur-Yvette Cedex, France*

[5]*Matériaux et Phénomènes Quantiques, MPQ, Université Denis Diderot–Paris 7, CNRS, UMR 7162 2 Place Jussieu, 75005 Paris, France*

(Received 27 February 2006; published 11 October 2006)

This study makes reference to the surface structure of MnAs(0001) epilayers grown by molecular beam epitaxy through a multitechnical method that combines scanning tunneling microscopy (STM), x-ray photoelectron spectroscopy (XPS), grazing incidence x-ray diffraction (GIXD), and *ab initio* calculations. Two surface reconstructions were studied, i.e., the (2×2) and the (3×1). Photoemission measurements provided quantitative information about (i) the surface coverage of both surfaces and (ii) the atomic environment of surface atoms. An atomic structural model has been proposed for the observed reconstructions. On the basis of STM observations and *ab initio* calculations the (2×2) phase is constituted by As trimers adsorbed on an underlying Mn layer of bulk MnAs, while x-ray diffraction analysis, coupled with STM, showed that the (3×1) reconstructed surface is constituted of long and narrow As chains aligned with the $\langle110\rangle$ GaAs substrate equivalent directions.

DOI: 10.1103/PhysRevB.74.155412 PACS number(s): 68.35.Bs, 68.55.−a, 68.37.Ef, 68.47.De

I. INTRODUCTION

The surface structures of MnAs epilayers grown on GaAs substrates have been studied by several groups in the last years.[1–6] MnAs is a ferromagnetic metal with a hexagonal structure ($P6_3/mmc$), NiAs type, $a=3.72$ Å, and $c=5.71$ Å. Since it grows epitaxially on GaAs(001) and GaAs(111)B, ferromagnetic metal/semiconductor heterostructures for "spintronics" could be realized. Recently, low temperature tunneling magnetoresistence (TMR) was reported for MnAs/GaAs/MnAs tunnel junctions.[7] The polarized injection efficiency remains however limited, due to a small density of defects in the semiconducting barrier that are created during the low temperature growth required to avoid interdiffusion. The defects work like deep-level impurities in the band gap, leading to a resonant tunneling magnetoresistance phenomenon. With the purpose of tailoring hybrid junctions and, in particular, to reduce the defect density in the III-V barrier, a better knowledge of the structure of interfaces and surfaces is still required. Indeed, the observed surface reconstructions of MnAs are driven by the surface stoichiometry[6] and, consequently, they can determine the interface stoichiometry of the MnAs/GaAs tunnel barrier. It has also been related that this latter parameter is of the highest importance for spintronic related studies.[2] Moreover, it was shown that only a 7 nm thick GaAs barrier covers completely the MnAs surface. Scanning tunneling microscopy (STM) observations of thinner GaAs barriers[8] revealed the presence of uncovered zones of MnAs that are detrimental to spintronics since they can generate pinholes. These uncovered regions could be easily identified after STM imaging since fingerprints of MnAs surface reconstructions had already been reported in Ref. 6.

The investigation reported in this paper is motivated by a better understanding of the atomic structures of the MnAs surface reconstructions. In Ref. 6 we had already reported the existence of three different surface reconstructions, i.e., the (3×1), the (2×2), and a mixture of phases $(2\times2)+(3\times1)$. The stability of each reconstruction was shown to be dependent of As covering of the surface. It was also shown that these surface reconstructions were stable at room temperature. *In situ* STM and reflection high energy electron diffraction (RHEED) measurements permitted us to put forward the hypothesis that the (3×1) reconstruction is composed of long and narrow As-constituted structures (chains), aligned with the $\langle110\rangle$ GaAs substrate's equivalent directions [see Figs. 1(a) and 2(a) of this paper]. This surface reconstruction is As richer than the (2×2) [Fig. 1(c)]. A mixture of phases $(2\times2)+(3\times1)$ [Fig. 1(b)] is also observed. Two surface atomic models were also proposed for the (2×2) reconstruction on the basis of STM analysis. Both models, presented below, show that this surface is As terminated but they diverge in respect to its atomic structure.[5,6] If STM measurements may supply useful indications about the surface structure of a given reconstruction, a more complete study remains unavoidable to confirm the validity of such models. In this paper we have combined STM, x-ray photoemission spectroscopy (XPS), and grazing incidence x-ray diffraction (GIXD) in order to determine the atomic structure of the (2×2) and (3×1) reconstructed surfaces. *Ab initio* calculations are also employed to determine the precise atomic structure of the (2×2) reconstruction.

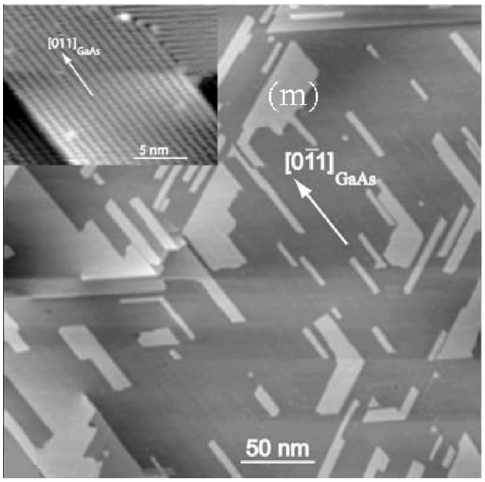

(a)

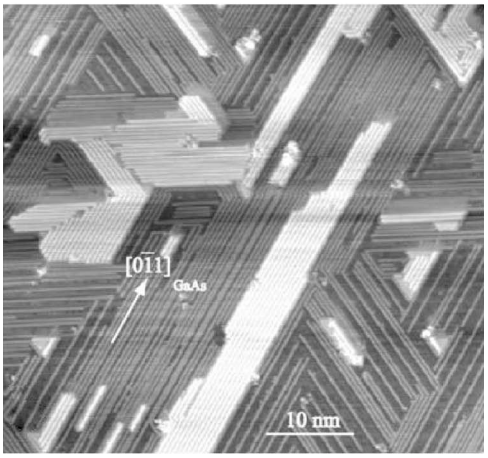

(b)

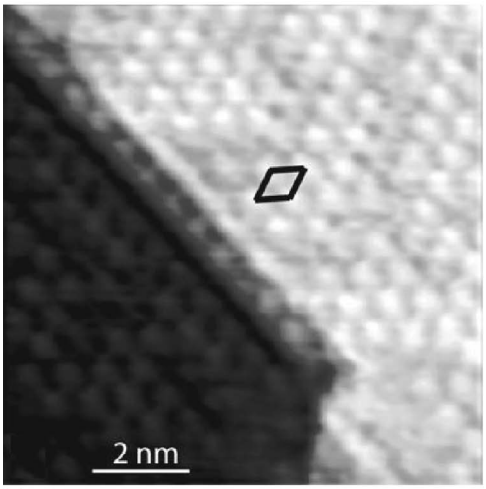

(c)

FIG. 1. STM images of the MnAs(0001) surface. The image was recorded at +1.895 V sample bias and 0.204 nA tunneling current. (a) The surface is (3×1) reconstructed; the point indicated by "*m*" is an As terrace; (b) mixture of phases $(2\times2)+(3\times1)$; (c) the surface is (2×2) reconstructed. As desorption by annealing leads the (3×1) towards the (2×2) reconstruction. White arrows indicate GaAs substrate directions. Insets are reported to show atomic features of the surfaces.

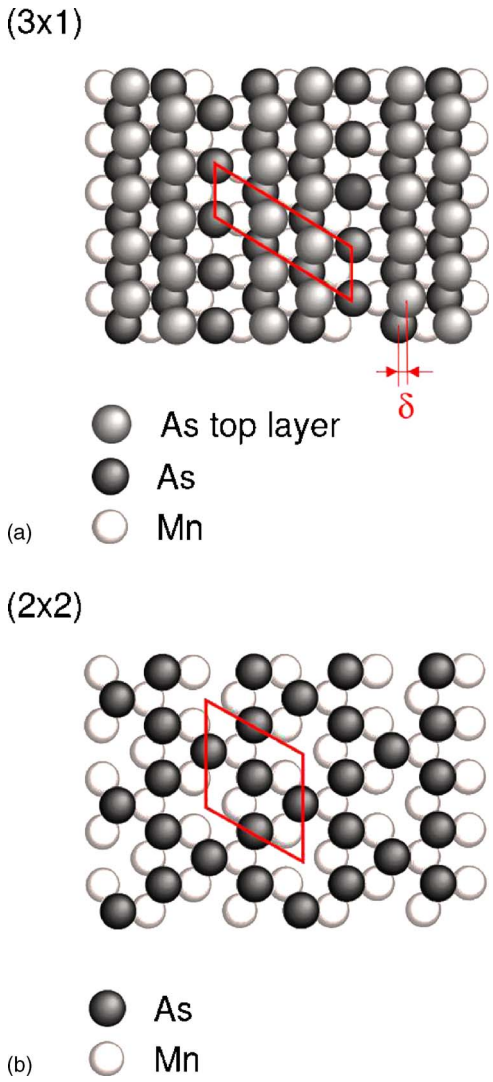

FIG. 2. (Color online) Structural atomic model for: (a) the (3×1) reconstructed surface and (b) the (2×2) surface reconstruction.

II. EXPERIMENTAL AND CALCULATION DETAILS

Growth. The MnAs epilayers were grown in a III-V molecular beam epitaxy (MBE) system on a GaAs(111)B substrate (Si-doped, 10^{18} cm^{-3}) with samples mounted with indium on a molybdenum plate.[6] The sample temperature was checked with a thermocouple placed at the back of the plate and double checked with an infrared pyrometer. Before the MnAs growth, a thin GaAs buffer layer was deposited at 580 °C under As-rich conditions. The streaky and intense RHEED pattern attested the flatness of the buffer layer, which displayed a $(\sqrt{19}\times\sqrt{19})R23.4°$ reconstructed surface during growth.[9] While cooling, the surface evolved to (2×2) below ~480 °C, when the As shutter was closed. The MnAs growth, performed at the substrate temperature of 280 °C, started by opening the As shutter followed after a few seconds by the Mn shutter. The epilayers investigated here were 100 nm thick and grown at a rate of ~2.5 nm/min. The epilayers displayed the epitaxial relations already described in Refs. 10 and 11: (0001)MnAs‖(111)GaAs-B and

$[\bar{2}110]$MnAs$\|[0\bar{1}1]$GaAs-B. The STM images were collected *in situ*.

Next, samples were transferred in a UHV portable chamber from the MBE chamber to the LURE-SUPERACO SB 7 beamline devoted to XPS studies. No C or O contaminations could be detected by XPS, attesting the efficiency of the UHV transfer. The photoemission measurements were carried out in a high resolution electron spectrometer (Scienta 2002) coupled with a Dragon monochromator. Spectra were collected in the normal emission mode; the total instrumental energy resolution was about 0.2 eV, as measured from the Fermi edge of a thick Fe film. The incidence angle of the photon beam was 45° off the normal surface.

The photoemission spectra of the two reconstructed surfaces were measured on the same sample. The initial (3×1)-reconstructed surface, stabilized in the MBE chamber before UHV transfer to the photoemission experimental setup, was carefully analyzed. Next, the surface was annealed under UHV until the appearance of a (2×2) surface following the procedure reported in Ref. 6.

The As-3*d* core level emissions of the (3×1) and (2×2) reconstructed surfaces were analyzed. Two photon energies (250 eV and 150 eV) were used in order to put into evidence surface contribution with respect to bulk and also to check for any undesired interference with Auger peaks. The electron escape depths (λ) were estimated at 6 ± 1 Å and 9 ± 1 Å for photon energies of 150 eV and 250 eV, respectively.

GIXD experiments were carried out to test the atomic arrangement of the (3×1) surface given in Ref. 6. Concerning the (2×2) surface reconstruction, the bulk contributions of the well known orthorhombic β-MnAs phase[11] overlapped with the fractional rods of the (2×2) reconstruction precluding atomic surface structural analysis. This lack of feasibility for surface structure determination motivated the complementary *ab initio* calculations on this surface that will also be presented in this paper.

The DW12 beamline at LURE-DCI was equipped with a MBE facility directly connected to a UHV *z*-axis diffractometer devoted to surface diffraction. The MnAs epilayers were grown with the same procedure already discussed before. After the growth, a low energy electron diffraction (LEED) survey of the (3×1) surface was performed and the sample transferred under UHV to the diffractometer. Data were collected with 15 keV monochromatic radiation, with the incident beam set at the critical angle for total external reflection ($\alpha=0.18°$). A total of 22 in-plane factionary order reflections and four factionary rods were measured. Data analysis and structural refinement were performed with the ANA and ROD codes supplied by Vlieg.[12] Corrections specific to the *z*-axis geometry of the instrument were applied to correct the geometrical factors.[13]

Ab initio calculations were performed to determine the atomic configuration of the (2×2) reconstructed surface. These calculations were based on density functional theory (DFT) (Ref. 14) to compute the energy of an As trimer added on a clean surface and forming a (2×2) reconstruction. Calculations were performed using the code PWSCF.[15] Spin-polarized DFT, which is an essential ingredient for the precise description of MnAs bulk,[16] was used. For the exchange and correlation potential, generalized gradient approximation (GGA) with the Perdew-Wang parametrization[17] was used. Pseudopotentials were generated according to the Vanderbilt scheme,[18] and the wave functions were expanded in plane waves up to a 30 Ry cutoff. The integration over the electronic states was performed using a Gaussian broadening of 0.02 Ry.[19] To simulate the surface, a supercell geometry approach was used. This comprised a slab of 5 layers with an in-plane periodicity corresponding to a (2×2) bulk unit cell. The same number of As atoms were added to each of the two surfaces of the slab so as to preserve the inversion symmetry along the *z* axis. The slabs were separated by 8 Å of vacuum. An integration grid of $6\times6\times4$ electronic **k** points was used, and all the atomic positions were relaxed until the force on each atom was less than 1×10^{-3} Ry/Bohr. The total number of atoms for a slab was 26, which corresponds to 14 As atoms plus 12 Mn. More details are given below.

III. RESULTS AND DISCUSSION

A. STM images

The MnAs(0001) surface reconstructions will be presented with the help of STM images. During growth the predominant surface reconstruction was (2×2) that remained stable when cooling down to room temperature. However, after the growth process, when the sample was cooled down to 200 °C under As overpressure, the surface evolved to a (3×1) reconstruction with three different domains rotated by 120° to preserve the substrate surface's symmetry. A mixed phase could also be stabilized for intermediary processes. The room temperature STM images in Fig. 1 show large scale areas of the (3×1)-reconstructed surface (As chains are visible in the inset), (b) the mixed phase $(2\times2)+(3\times1)$, and (c) the (2×2) surface. After the monitoring of the RHEED patterns' evolution from the (3×1) to the (2×2) surface induced by a small Mn flux, it was possible to establish that 1.5 ML of Mn is required to induce this transition. This experiment provided a quantitative stoichimetry difference between both surfaces. With the help of atomic resolved STM images we advanced some hypotheses about the atomic structure of these two surfaces.[6]

The (3×1)-reconstructed surface model is based on the bulk As atomic structure. Indeed, the structural similarities between rhombohedral bulk arsenic ($a=3.76$ Å, $c=10.55$ Å) (Ref. 20) and MnAs ($a=3.72$ Å, $c=5.71$ Å) supports the structure proposed in Fig. 2(a). Topmost As atoms occupy positions close to the bulk As lattice on top of an hexagonal As layer [the As-terminated bulk truncated MnAs (0001) plane]. The difference is that only 2 atoms occupy the three sites of the surface unit cell [see Fig. 2(a)] that corresponds to a final arsenic coverage of 1.67 ML.[6] This model is in agreement with STM images [see inset of Fig. 1(a)], where As chains are aligned along the $\langle110\rangle$ GaAs substrate directions with a period of 9.7 Å.

Considering now the (2×2)-reconstructed surface [Fig. 1(c)], previous studies suggest that when epilayers are grown under As-rich conditions, white protrusions of the

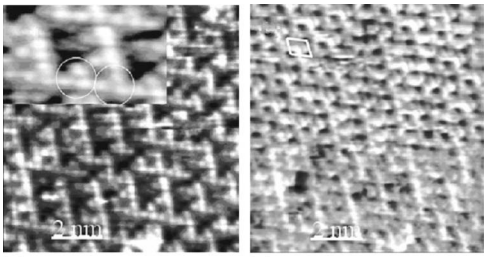

FIG. 3. STM images of the MnAs (0001) (2×2) reconstruction. The image (a) was recorded at −0.527 V sample bias and 0.09 nA and the image (b) at 0.152 V sample bias and 0.09 nA. The white lozenge evidences the (2×2) primitive surface cell. Inset: atomic resolution of trimers on the surface.

(2×2)-reconstructed surface correspond to As atoms resulting in two proposed atomic models. One model makes reference to As trimers lying on an As terminated surface[5] [similarly to the (2×2)-reconstructed GaAs(111) surface of Ref. 9]. It is worthwhile pointing out that this model works in an As coverage of 1.75 ML. This is higher than the (3×1) model proposed above and it is at odds with the RHEED measurement that results in a (3×1) As coverage higher than the (2×2). The latter suggests that only one As atom in the surface unit cell lies on a Mn terminated surface (ad-atom model).[6] An improved atomic resolution could be achieved after performing a UHV annealing of the sample at 300 °C. Figures 3(a) and 3(b) show such images collected simultaneously *with both positive and negative bias* (forwards $V=-0.527$ V, $I=0.09$ nA; backwards $V=0.152$ V, $I=0.09$ nA). A careful observation of the main features of the two images reveals that the white objects of Fig. 3(b) are still white in Fig. 3(a), i.e., no color contrast is observed. Since white protrusions correspond to As-constituted structures[6] and contrast does not depend on the applied voltage, we conclude that the three atoms, clearly detectable in the unit cell surface [see inset in Fig. 3(a)], are As atoms.

After these observations the atomic model of the (2×2) surface is presented in Sec. III C. This model is obtained by a combined XPS and *ab initio* calculations' study.

In Sec. III B XPS and GIXD's combined study of the (3×1) surface is presented. It appears that (i) the structural model previously proposed[6] is corroborated by the present GIXD measurements and (ii) a better chemical understanding of this surface is achieved by XPS.

B. The XPS and GIXD results on the (3×1) surface

1. Core levels

The experimental As 3*d* spectra and their fitting are reported in Fig. 4 for the (3×1) surface. Three contributions have to be considered to obtain consistent fits using a least-square fitting procedure: two arising from the surface (*S*1,*S*2) and the bulk one. We found that the extra *S*1 and *S*2 components are shifted towards higher binding energies with respect to the bulk component. The origin and the chemical shift of these two *S*1 and *S*2 components are discussed later in the text.

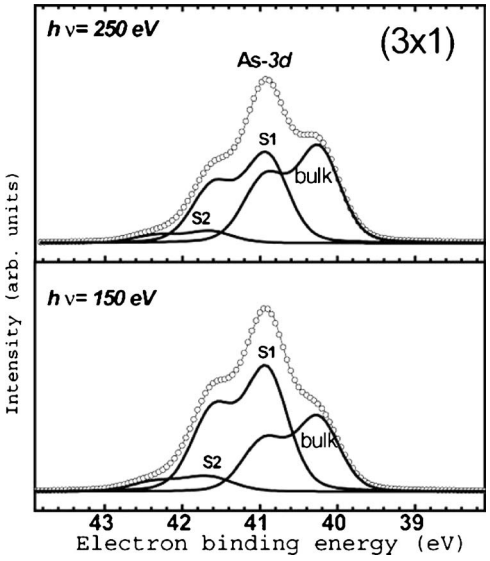

FIG. 4. XPS spectra of the As 3*d* core level from the MnAs (3×1) surface taken at two photon energies (250 eV and 150 eV). For each spectrum we give the experimental data after background subtraction and the decomposition with bulk and two surfaces components identified by *B*, *S*1, and *S*2, respectively.

The components are spin-orbit pairs with symmetric Voigt line shape: the energy split and branching ratio are fixed at 0.68 eV and 1.5, respectively.[21] The Lorentzian contribution to the Voigt profile is about 20% of the full width at half the maximum (FWHM) of As $3d_{3/2}$ and As $3d_{5/2}$ peaks. The Gaussian width required to fit spectra is significantly broader than the expected experimental resolution, indicating probably an influence of disorder and/or of the surface potential (see Refs. 22 and 19). The chemical shift of all components with respect to the volume and their relative intensity are given in Table I for both surface reconstructions and photon energies.

Both *S*1 and *S*2 components show larger intensity ratio with respect to the bulk component when a more surface sensitive energy is used (150 eV). This justifies their attribution to surface components.

First, surface coverage will be evaluated in regard to the relative intensities of the surface peaks with respect to the bulk component.

In Table I we can notice that the (3×1) surface gives a $S1/B$ ratio equal to 0.93 and 1.7 for incoming photon ener-

TABLE I. Parameters used in fitting the experimental data of the As 3*d* core level for two reconstructed surfaces (in Figs. 4 and 7). The procedure used in the fitting is described in the text.

Surface reconstruction:	(3×1)		(2×2)	
Photon energy:	150 eV	250 eV	150 eV	250 eV
Shift binding energy (*S*1-*B*)	0.64	0.64	0.48	0.48
Shift binding energy (*S*2-*B*)	1.4	1.4	1.4	1.4
% area bulk intensity (*B*)	34	49	75	80
% area surface intensity (*S*1)	58	45.5	18	15
% area surface intensity (*S*2)	8	5.5	7	5

gies of 250 eV and 150 eV, respectively. A simple simulation of the exponential decay expected for the bulk contribution (B) as a function of the surface covering (the $S1$ contribution) and of the electron escape depths λ (estimated at 6±1 Å and 9±1 Å for photon energies of 150 eV and 250 eV, respectively) can give a coarse evaluation of the surface coverage. The measured experimental ratio, $R=S1/B=1.7$ at 150 eV and 0.93 at 250 eV, fit well with the expected values obtained by an exponential decay of roughly 2 ML of As covering a Mn-terminated surface. Thus, the As coverage deduced by XPS corroborates the atomic structural model of the (3×1)-reconstructed surface already proposed in Ref. 6. This model, displayed in Fig. 2(a), presents an arsenic content of about 1.67 ML.

Another important piece of information concerns the chemical shift observed for $S1$ and $S2$ components that can be attributed to the presence of As atoms in As-As environments. Since arsenic has a larger electronegativity than Mn (2.18 and 1.55 in the Pauling scheme), the binding energy of As-3d photoelectrons is expected to be lower in Mn-As than in As-As environments. In short, the energy shifts of $S1$ and $S2$ can be interpreted in the following manner: the richer the As environment, the larger its binding energy.

The other surface contribution ($S2$), detected at higher binding energies (+1.4 eV), represents 8% of the intensity of the As3d peak, corresponding to less than 0.5 ML. The origin of the $S2$ component is attributed to As-crystalline islands that are frequently observed in STM images [indicated by "m" in Fig. 1(a)]. The surface preparation procedure, with high arsenic fluxes at low substrate temperatures can promote such an As crystallization, probably in defective surface regions. This very rich As environment leads to a large binding energy.

2. Grazing incidence x-ray diffraction experiments

GIXD measurements were carried out in order to test the structural model previously proposed for the MnAs(0001) (3×1) surface and to further understand its atomic structure. The crystallographic basis vectors for the surface unit cell can be given by following the three or four indexes' conventions. They are related to the hexagonal bulk basis of $\mathbf{a}_{surf}=[100]$ or $[\bar{2}110]$, $\mathbf{b}_{surf}=[010]$ or $[1\bar{2}10]$, $\mathbf{c}_{surf}=[001]$ or $[0001]$. The in-plane directions are spanned by the Miller indices H and K along the a^* and b^* reciprocal crystal axes. The out-of-plane direction is taken to be the c axis, which is always the same direction as c^*, and the perpendicular component of the momentum-transfer vector is denoted by the index L. The scans performed along the H and K directions displayed a "×3" periodicity corresponding to the three (3×1) reconstructed domains, in agreement with STM measurements [see Fig. 1(a)] both the super-period of the (3×1) reconstruction and the half-order peaks characteristic of the orthorhombic phase as already mentioned (bulk crystal truncation rods). The integrated intensity was obtained by rocking scans of the available surface reconstruction reflections. After correction by Lorentz factor, polarization, and illuminated surface area, this experimental data set has been used to test and refine the surface structural model, using a least square routine with a minimum of adjustable parameters. The quality of the fitting procedure was determined by the R factor defined as:

$$R=[\Sigma(|F_{HKL}(\text{exp})-F_{HKL}(\text{cal})|)]/\Sigma[F_{HKL}(\text{exp})].$$

$F_{HKL}(\text{exp})$ is the measured structure factor for the HKL reflection, taken as the square root of the integrated intensity and F_{HKL} (cal) is the calculated structure factor for the HKL reflection. The starting structural model, shown in Fig. 2(a), is formed by a bulklike As-terminated MnAs surface with an As extra-layer added following the hexagonal symmetry and with the As atoms occupying the $H3$ positions. This overlayer is not fully occupied since one out of three As atoms of the top layer are missing, leading to the formation of rows. Surprisingly, this simple model without any other adjustable parameter, except a scaling factor, reproduces the overall intensities for the in-plane data with an R of about 0.2 (see Fig. 5). Considering first the in-plane displacements, only one parameter (plus the scaling factor) has been found to be significantly shifted from the expected position for this packing. We have expressed the position of this extra surface overlayer by its position δ with respect to the bottom bulklike terminated As layer [Fig. 2(a)]. The δ value is of 0.107 nm for a perfect hexagonal packing while we have obtained a δ of 0.06 nm after structural refinement. This displacement dropped R to about 0.1, which is a very good value considering the few adjustable parameters. In a similar way the out-of plane rods, without any adjustable parameter, reproduce the intensity modulation period along L although the origin is found shifted. With the refinement of the averaged distance between the two upper As layers, the fit improves (Fig. 6). The agreement is not perfect but the general trend points to a real structure not very far from this simplistic model. The difficulty to go further with the refinement concerns the number of variables required to fully determine the positions of different atoms. In fact, the lack of symmetry of the surface unit cell and its size introduce too many independent parameters with respect to the available data.

Comparing in-plane data with the model (Fig. 5) one can say that the surface projection of this STM/XPS proposed model agrees well with a suitable R value of 0.1 and with a small number of adjustable parameters. The out-of-plane agreement is less evident but it verifies the coherence of this

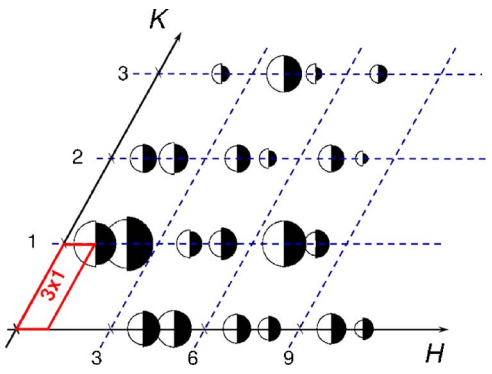

FIG. 5. (Color online) Comparison between experimental in-plane GIXD data and calculated structure factors.

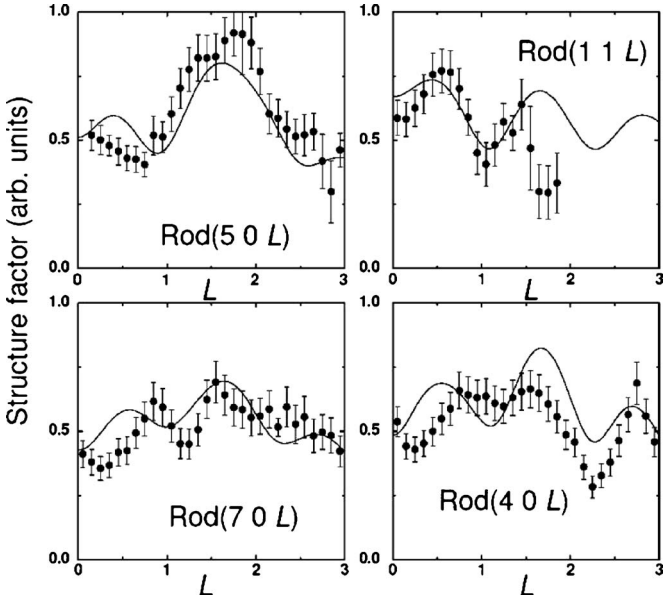

FIG. 6. Comparison between experimental GIXD data and calculated structure factors for reconstruction related rods. The vertical bars indicate the experimental errors.

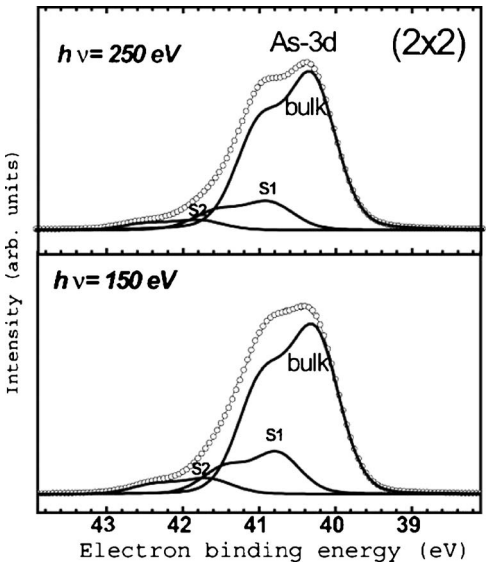

FIG. 7. XPS spectra of the As 3*d* core levels from the MnAs (2×2) surface taken at two photon energies (250 eV and 150 eV). For each spectrum we give the experimental data after background subtraction and the decomposition with bulk and two surface components identified by *B*, *S*1, and *S*2, respectively.

model considering the single out-of-plane structural adjustable parameter. A graphic representation of the measured and calculated structure factors for the (3×1) model is presented in Fig. 5. The adjustment gives an in-plane As-As distance of 0.372 nm, similar to the distance in MnAs. The distance between this extra-arsenic plane and the adjacent As layer is found to be a little expanded, with 0.18 nm compared with the As-Mn distance of 0.143 nm. This expansion can be justified either by the truncation of the surface and/or by the different chemical bond between As-As and As-Mn.

C. The (2×2) reconstructed surface: XPS and *ab initio* calculations

1. Core levels

A similar study has been performed with the (2×2) reconstructed surface with As-3*d* core levels spectra being recorded and fitted within the same procedure as previously reported for the (3×1) reconstruction.

Two surface components (*S*1 and *S*2) were necessary to obtain a good and trustworthy fit of the XPS As-3*d* signal (Fig. 7). Considering the binding energy similarities with the *S*1 and *S*2 components of the (3×1) surface, we were tempted to maintain the same notations as before. Not surprisingly, the intensity of surface peaks was reduced with respect to the (3×1) reconstruction (see Table I). At 150 eV, the *S*1 and *S*2 components represent only 18% and 7%, respectively. We followed the coverage evaluation procedure described above for the (3×1) reconstruction. The experimental ratios (0.24 and 0.1875 at 150 eV and 250 eV, respectively) attest that As coverage ranges between 0.5 ML and 1 ML. This coverage is incompatible with the As-trimers model, i.e., As-trimers are bonded to an As-terminated surface (1.75 ML). Moreover, it gives an As amount slightly richer than the ad-atoms model of Ref. 6 where only 0.25 ML of As is adsorbed on a Mn-terminated surface in their bulksite (ad-atoms model).

Concerning the *S*2 component, a similar behavior as in the (3×1) surface is observed, remembering that the presence of this component has been attributed to crystalline As islands that condensate during the preparation of the (3×1) surface. We have observed in some STM images (not shown) that As-crystalline islands can persist even for the (2×2) surfaces, whenever this surface is obtained by UHV annealing of the initial prepared (3×1) reconstructed surface.

It is also important to notice that no extra component that could be a mark of As-Mn surface bond was observed. We suspect that this contribution remains probably masked within the bulk MnAs components.

Now, we want to address some comments about the chemical shift observed for the (2×2) reconstructed surface. An interpretation can be derived from previous detailed studies of the (2×2) reconstructed surfaces for GaAs(111)A and GaAs(111)B (Ref. 22) where As structures are found on the surface. The high binding energy (HBE) surface component of As 3*d* core levels was attributed to As atoms in a rich As environment (shift of +0.47 eV with respect As bulk in GaAs). Similarly, we attribute the observed HBE MnAs-components (*S*1 and *S*2 in Figs. 4 and 7) to an As-rich environment on the surface. These considerations (coverage plus the As environment) lead us to conclude that the trimers visualized in STM images on the (2×2)-reconstructed surface are formed by As atoms lying on a bulklike Mn-terminated top layer.

It is worthwhile noticing that the *S*1 component of the (3×1) and (2×2) reconstructions are found at very similar binding energies: 0.64 eV and 0.48 eV, respectively. Since

the (3×1) surface has a $\sim$1 ML As-richer coverage, the richer As environment leads to the observed larger binding energy. In other words, the (3×1)-reconstructed surface presents an As environment closer to the bulklike As.

2. Ab initio calculations

The results presented here bring us to the conclusion that the (2×2) reconstruction is formed by As trimers on a clean Mn bulklike surface. Nevertheless the exact structure of these trimers cannot be determined by STM and XPS measurements. To complete this gap, calculations were performed using three different slabs corresponding to different positions of the trimer. The trimer was assumed to be: (i) on the bulk As sites, (ii) on the top of the topmost Mn atom, and (iii) on the bulk As antisites (on the top of the second As layer below). These three slabs have in common the same coverage (0.75 ML) and their relative stability can be determined by comparing the calculated values for the total energy. It results that the most stable configuration is, by far, the one (i) presented in Fig. 2(b), with an energy gain of 4.6 eV/unit cell and 1.1 eV/unit cell with respect to (ii) and (iii). At equilibrium, for the configuration (i), the As trimer atoms occupy a slightly displaced position, with As-As distance contracted to 3.63 Å, in agreement with STM images. The distance between the As surface and the underlying nearest Mn neighbor atomic plane is reduced from 2.55 Å to 2.50 Å. The stability of the (2×2) reconstruction with respect to the unreconstructed (1×1) surface as a function of the chemical potential will be presented elsewhere.[23]

IV. CONCLUSIONS

We have investigated the structure of two stable surface reconstructions of MnAs (0001) epilayers, i.e., the (2×2) and the (3×1). A multitechnical approach has been used combining scanning tunneling microscopy (STM), x-ray photoemission (XPS), grazing incidence x-ray diffraction (GIXD), and *ab initio* calculations.

GIXD results confirm that the structure of the (3×1)-reconstructed surface is composed of a pile of long and narrow structures aligned along the $\langle110\rangle$ GaAs substrate equivalent directions. Atoms are disposed in a hexagonal symmetry with the As atoms occupying *H*3 positions. This overlayer is not fully occupied since one over three As atoms of the top layer is missing leading to the formation of rows with slight surface induced in-plane relaxation. The surface coverage, determined by XPS, indicates that these structures are constituted of two layers of As atoms covering a Mn-terminated MnAs surface. These structures can be interpreted as rhombohedral arsenic crystallizing on a Mn-terminated surface.

Concerning the (2×2) reconstructed surface, STM images show the presence of three atoms in a patch of trimers for the (2×2)-reconstructed surface. This surface is As poorer than the (3×1) since surface components of As-3*d* peaks obtained by photoemission measurements reveal that these trimers are As constituted and lie on a Mn-terminated surface. *Ab initio* calculations reveal that As atoms constituting trimers are located close to the As bulk positions leading to an As-As distance of 3.63 Å and are stable if compared to the (1×1)-unreconstructed surface.

ACKNOWLEDGMENTS

Calculations were performed at the IDRIS Supercomputing Center (Orsay, France) within the Project 20050911820.

*Present address: Laboratoire de Photoniques et de Nanostructures, LPN-CNRS (UPR 20) Site Alcatel de Marcoussis Route de Nozay, 91460 Marcoussis, France.

†Also at Programa de Pós-Graduação em Engenharia—UFPR, Centro Politécnico, Prédio da Administração 2° andar -Jardim das Américas, Cx.P.: 19011—CEP.: 81531-990. Curitiba—PR, Brazil.

[1] J. Sadowski, J. Kanski, L. Ilver, and J. Johansson, Appl. Surf. Sci. **166**, 247 (2000).
[2] M. Tanaka, K. Saito, and T. Nishinaga, Appl. Phys. Lett. **74**, 64 (1999).
[3] F. Schippan, M. Kästner, L. Däweritz, and K. H. Ploog, Appl. Phys. Lett. **76**, 834 (2000).
[4] V. H. Etgens, M. Eddrief, D. Demaille, Y. L. Zheng, and A. Ouerghi, J. Cryst. Growth **240**, 64 (2002).
[5] J. M. Kästner, L. Däweritz, and K. H. Ploog, Surf. Sci. **511**, 323 (2002).
[6] A. Ouerghi, M. Marangolo, M. Eddrief, S. Guyard, V. H. Etgens, and Y. Garreau, Phys. Rev. B **68**, 115309 (2003).
[7] V. Garcia, H. Jaffrès, M. Eddrief, M. Marangolo, V. H. Etgens, and J. M. George, Phys. Rev. B **72**, 081303(R) (2005).
[8] V. Garcia, M. Marangolo, M. Eddrief, H. Jaffrès, J. M. George, and V. H. Etgens, Phys. Rev. B **73**, 035308 (2006).
[9] D. K. Biegelsen, R. D. Bringans, J. E. Northrup, and L. E. Swartz, Phys. Rev. Lett. **65**, 452 (1990).
[10] M. Tanaka, J. Cryst. Growth **201-202**, 660 (1999).
[11] N. Mattoso, M. Eddrief, J. Varalda, A. Ouerghi, D. Demaille, V. H. Etgens, and Y. Garreau, Phys. Rev. B **70**, 115324 (2004).
[12] E. Vleig, J. Appl. Crystallogr. **33**, 401 (2000).
[13] O. Robach, Y. Garreau, K. Aïd, and M. B. Véron-Juilliot, J. Appl. Crystallogr. **33**, 1006 (2000).
[14] P. Hohenberg and W. Kohn, Phys. Rev. **136**, B864 (1964); W. Kohn and L. J. Sham, Phys. Rev. **140**, A1133 (1965).
[15] S. Baroni, S. de Gironcoli, A. Dal Corso, and P. Giannozzi, http://www.pwscf.org
[16] A. Debernardi, M. Peressi, and A. Baldereschi, Comput. Mater. Sci. **27**, 175 (2003).
[17] J. P. Perdew and Y. Wang, Phys. Rev. B **45**, 13244 (1992).
[18] D. Vanderbilt, Phys. Rev. B **32**, 8412 (1985).
[19] C. J. Spindt, M. Yamada, P. L. Meissner, K. E. Miyano, T. Kendelewicz, A. Herrera-Gomez, W. E. Spicer, and A. J. Arko, Phys. Rev. B **45**, 11108 (1992).
[20] D. Schiferl and C. S. Barret, J. Appl. Crystallogr. **2**, 30 (1969).
[21] This value is the same value usually used for As 3*d* core level in GaAs. No change in fitting results was observed when the spin-orbit separation was varied in a ±0.01 eV range.
[22] J. M. C. Thornton, P. Weightman, D. A. Woolf, and C. J. Dunscombe, Phys. Rev. B **51**, 14459 (1995), and references therein.
[23] M. Lazzeri and M. Marangolo (unpublished).